

# EFFECT OF SURFACE ROUGHNESS ON THE PRESSURE GENERATION IN A FINITE ROUGH HYDRODYNAMIC JOURNAL BEARING UNDER MICROPOLAR LUBRICATION IN STEADY-STATE CONDITION

**Gautam Kumar<sup>1</sup>, Sujeet Kumar Jha<sup>2</sup>, Ujjal Baidya<sup>3</sup>, Santanu Das<sup>4</sup> and Sanjoy Das<sup>5\*</sup>**

<sup>1</sup>Govt. Polytechnic, Lakhisarai, Bihar

<sup>2</sup>Technosoft Electronics Pvt. Ltd., Mumbai

<sup>3,5</sup>Department of Engineering and Technological Studies, University of Kalyani, Kalyani, West Bengal

<sup>1,2,4</sup>Department of Mechanical Engineering, Kalyani Government Engineering College, Kalyani, West Bengal

Email: <sup>1</sup>gautamsparky@gmail.com, <sup>2</sup>sjha1211@gmail.com, <sup>3</sup>baidya.ujjal@gmail.com, <sup>4</sup>sdas.me@gmail.com,

<sup>5</sup>dassanjoy0810@hotmail.com

\* Corresponding author

**Paper received on: October 18, 2016, accepted after revision on: July 20, 2017**

**DOI:10.21843/reas/2016/39-53/158775**

**Abstract:** In hydrodynamic lubrication of journal bearing pressure of the fluid film is generated as a result of the viscous drag of the fluid into the wedge shaped gap between the journal and bearing due to relative motion of the journal with respect to the bearing. The pressure development of fluid is important in this type of lubrication to ensure performance of journal bearing. On the other hand, every surface has some degree of roughness that affects relative motion of the journal bearing system. This paper, thus, aims to present a detailed study of hydrodynamic pressure built up of a journal bearing including the roughness of the surfaces. The modified Reynolds equation is derived on the basis of theory of micropolar lubrication incorporating suitable roughness model. The resulting equation is solved numerically at steady state operating condition using cavitation boundary condition to observe distribution of pressure. The effects of variations in operating variables in terms of characteristic of lubricant and parameters defining roughness model are computed. The analytical results are compared with the available published results to validate the theory and computer code. The numerical result shows that for same geometrical condition maximum pressure developed in micropolar fluid always remain higher than that in Newtonian fluid. The steady state pressure is found to be decreased as the values of the roughness parameters are increased.

**Keywords:** Hydrodynamic Bearing, Micropolar Lubrication, Roughness, Steady state, pressure profile

## NOMENCLATURE

$C$	Radial clearance.	$\bar{h}$	Non-dimensional steady state film thickness, $\bar{h} = \frac{h}{C}$ .
$\epsilon_d$	Eccentricity ratio.	$H$	Steady state film thickness considering roughness of journal bearing.
$\bar{F}(N, l_m, \bar{h}, \bar{\alpha}, \bar{\sigma}, \bar{\xi})$	Non-dimensional micropolar fluid function.	$\bar{H}$	Non-dimensional steady state film thickness considering roughness of journal bearing $\bar{H} = H/C$ .
$g(\lambda, N, H)$	Micropolar fluid function		
$h$	Steady state film thickness.		

EFFECT OF SURFACE ROUGHNESS ON THE PRESSURE GENERATION

$\bar{H}_{cav}$	Non-dimensional steady state film thickness corresponding to the cavitation considering roughness of journal bearing.	$\theta$ $\theta_1, \theta_2$	Circumferential coordinate. Circumferential coordinates where the fluid film starts and cavitates respectively, (rad).
$l_m$	Non-dimensional characteristic length of the micropolar fluid, $l_m = A/C$ .	$U$ $V$	Velocity of journal, $U = \omega R$ . Velocity vector, $[L T^{-1}]$ (m/s).
$N$	Coupling number, $N = \left( \frac{\chi}{2\mu + \chi} \right)^{\frac{1}{2}}$	$v$ $\alpha$	Microrotational velocity vector, $[L T^{-1}]$ (m/s). Mean surface roughness.
$p$	Micropolar film pressure in the film region.	$\bar{\alpha}$	Non-dimensional mean surface roughness, .
$\bar{p}$	Non-dimensional micropolar film pressure in the film region, $\bar{p} = \frac{pC^2}{\mu \omega R^2}$ .	$\sigma$ $\bar{\sigma}$	Standard deviation of roughness pattern. Non-dimensional standard deviation of roughness pattern, .
$R$	Radius of the journal.	$\xi$	Skewness of surface roughness.
$x$	Cartesian coordinate axis along the circumferential direction.	$\bar{\xi}$	Non-dimensional skewness of surface roughness,
$z$	Cartesian coordinate axis along the bearing axis.		
$\bar{z}$	Non-dimensional Cartesian coordinate axis along the bearing axis, $\bar{z} = \frac{z}{(L/2)}$		
$\chi$	Spin viscosity of micropolar fluid.		
$A$	Characteristic length of the micropolar fluid.		
$\mu, \lambda$	Newtonian viscosity coefficients.		
$\omega$	Angular velocity of the journal.		

**1. INTRODUCTION**

The rapid technological advancements and the increasing operating speed of machines in recent days demand more exact and realistic bearing characteristic data for the design of the bearings. The hydrodynamic lubrication in rotating bodies is advantageous due to its self ability to develop high pressure. The mechanism of hydrodynamic lubrication was first explained by Osborne Reynolds. The fluid used for lubrication of machine in general industrial conditions gets contaminated with dust and wear out particles. Sometimes external additives which are generally long-chained carbon polymers are added with the fuel as lubricant. In those cases the behavior of the lubricant can more clearly be explained with the

concept of micropolar fluid rather than the Newtonian lubrication theory, as developed by Eringen[1] and applied by other researchers[1-5]. In such fluids the added sub-structures undergo translational and rotatory motions generating a spin viscosity ( $\chi$ ) apart from the Newtonian viscosity ( $\mu$ ) and gyroscopic viscosity ( $\gamma$ ). As a result the lubricant shows an effective enhanced viscosity equals to  $(\mu + \frac{\chi}{2})$ . This enhances the load capacity but decreases the friction parameter in smooth straight hydrodynamic journal bearings [2, 5, 7]. However as no surface can be manufactured perfectly smooth journal surface and bearing inner surface always have some microirregularities. Theoretical analysis of rough surface in lubrication was first investigated by Hamilton et. al. [7] and he presented a theory that depicted hydrodynamic lubrication within two parallel surfaces having roughness on one or both. The theoretical and experimental results verified that surface roughness helped the pressure generation between the surfaces and maintained the sufficient load to keep the surfaces from direct collapsing. Christensen [8] in 1969 presented two separate models of hydrodynamic lubrication for rough bearing surfaces based on stochastic concept. The models were associated with one dimensional roughness one in longitudinal direction and the other in transverse direction. The study exhibited that the operating characteristic of a bearing became more affected by the surface roughness as the surfaces were brought closer together, conversely the effect of the roughness become insignificant when sliding surfaces were kept at an average separation larger than the roughness amplitudes. Christensen and Tonder [9] in their analysis of hydrodynamic lubrication for a finite width bearing using a stochastic surface roughness theory commented that the surface roughness might have beneficial or adverse effect on load capacity or friction parameter. Guha [10] investigated on the effect of isotropic roughness on steady state characteristic of a hydrodynamic journal bearing system having misalignment. He observed

increased roughness parameter to result in lowering of load capacity. Cheng & Chien [11] worked on linear stability of a journal bearing having short length considering the influence of surface roughness and flow rheology. They concluded rough journal bearing (except transverse roughness) to provide higher stability than that having highly finished surface. The study of Rao et. al. [12] on the effect of surface roughness on a porous inclined hydrodynamic slider bearing lubricated with couple stress fluid established that for the consideration of bearings life period the surface roughness needs be considered during bearing system design. However, in general the roughness is basically categorized into three patterns viz. longitudinal, transverse and isotropic. Longitudinal pattern offers less resistance to flow, whereas transverse roughness offers more resistance to flow and is better for pressure development for sealing devices, and finally the isotropic roughness is equally good for lubricant flow and hydrodynamic action [13]. Under mixed elastohydrodynamic lubrication for point contact, Yan et. al. [14] explored the influence of skewness and kurtosis on fatigue life of a material. It showed a drop in film thickness with increased skewness. Possible reason behind this may be that a negative skewness produces more flat surface with some deep valleys which after being filled up with lubricant, may have provided higher film thickness on an average. Oppositely a surface having positive values of the skewness is flatter with random peaks which disrupt the development of fluid film.

Though in all previous studies the roughness models were considered stochastic, especially being represented in the terms of mean, standard deviation and skewness, however no literature were found available that explicitly presented the effect of variation of those statistical parameters on hydrodynamic pressure generation.

The goal of this analysis is, thus, limited to study the expected steady state pressure profile by

solving the modified Reynolds equation using technique of finite difference method with appropriate boundary condition and to present the pressure generation for different parametric condition of lubricating fluid as well with respect to the variation of the statistical properties of the roughness model.

In this study the fluid flow is considered as incompressible, laminar, and isothermal and satisfies other assumptions of hydrodynamic lubrication. As the surface roughness is random in nature, the computed pressure profile is also a

random quantity. Asymmetric probability density function is assumed for the random variable that characterizes surface roughness with non-zero mean.

**2. ANALYSIS**

A hydrodynamic journal bearing in the circumferential coordinate system (shown in Fig. 1) is used in this analysis.

The modified Reynolds equation of a hydrodynamic journal bearing under micropolar lubrication in steady-state condition becomes [6]:

$$\frac{\partial}{\partial x} \left\{ g(\Lambda, N, H) \frac{\partial p}{\partial x} \right\} + \frac{\partial}{\partial z} \left\{ g(\Lambda, N, H) \frac{\partial p}{\partial z} \right\} = 6U \frac{\partial H}{\partial x} \tag{1}$$

Where,  $g(\Lambda, N, H) = \frac{H^3}{\mu} \left( 1 + 12 \frac{\Lambda^2}{H^2} - 6 \frac{N\Lambda}{H} \coth \frac{NH}{2\Lambda} \right)$  and  $H$  is the lubricant film thickness.

Incorporating the surface roughness the thickness of the fluid film for a hydrodynamic journal may

be represented as follows:

$$H(\theta) = h(\theta) + h_s \tag{2}$$

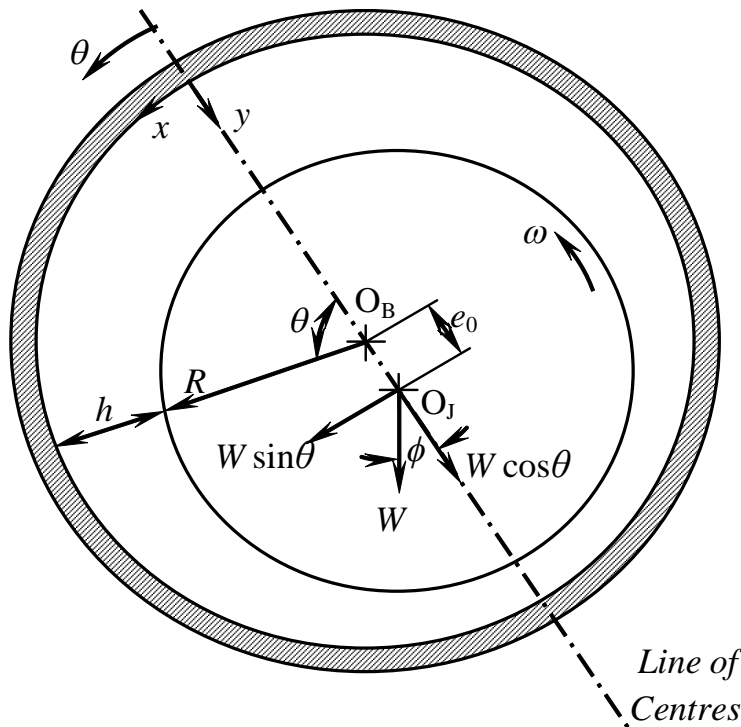


**Fig. 1 Schematic diagram of geometrical configuration of journal bearing system.**

Where,  $h(\theta) = C(1 + \varepsilon_0 \cos \theta)$ , represents the average fluid film thickness,  $C$  is the radial clearance,  $\varepsilon_0 = e_0/C$ , is the eccentricity ratio. The effect of roughness of the bearing surface is incorporated in the fluid film by adding stochastic film thickness ( $h_s$ ) measured from mean level of film thickness.  $f(h_s)$  represents the probability density function of  $h_s$  defined over the domain  $-C_s \leq h_s \leq +C_s$ , where  $C_s$  is the maximum deviation of film thickness from its mean. The mean ( $\alpha$ ), standard deviation ( $\sigma$ ) and skewness ( $\xi$ ) representing the nature of random variable  $h_s$  is defined as [11].

$$\left. \begin{aligned} \text{Mean, } \alpha &= E(h_s) \\ \text{Standard deviation, } \sigma^2 &= E[(h_s - \alpha)^2] \\ \text{Skewness, } \xi &= E[(h_s - \alpha)^3] \end{aligned} \right\} \quad (3)$$

Where,  $E(\cdot)$  represents the expectancy operator and is defined as:

$$E[f(x)] = \int_{-\infty}^{+\infty} f(x)f(h_s)dh_s = \int_{-C_s}^{+C_s} f(x)f(h_s)dh_s \quad (4)$$

This function terminates at  $C_s = 3\sigma$  where  $\sigma$  represents the standard deviation.

Now multiplying both side of eq. (1) by  $f(h_s)$  and integrating with respect to  $h_s$  in the limit  $-C_s$  and  $+C_s$  and  $E(H) = \bar{h} + \alpha$ ,  $E(p) = \bar{p}$  and  $\alpha$  being the mean of surface roughness does not vary with either time or position, the modified Reynolds equation becomes as follows:

$$\frac{\partial}{\partial x} \left\{ F(\Lambda, N, H) \frac{\partial p}{\partial x} \right\} + \frac{\partial}{\partial z} \left\{ F(\Lambda, N, H) \frac{\partial p}{\partial z} \right\} = 6\mu U \frac{\partial h}{\partial x} \quad (5)$$

In which

$$F(\Lambda, N, H) = \mu[G(\Lambda, N, H)] \\ = \frac{1}{\mu} \left[ \int_{-C_s}^{+C_s} H^3 f(h_s) dh_s + 12\Lambda^2 \int_{-C_s}^{+C_s} H f(h_s) dh_s - 6N\Lambda \int_{-C_s}^{+C_s} H^2 \coth \frac{NH}{2\Lambda} f(h_s) dh_s \right] \quad (6)$$

Eq. (6) with the following non-dimensionalisation scheme becomes:

$$\theta = \frac{x}{R}, \quad \bar{z} = \frac{z}{(L/2)}, \quad \bar{h} = \frac{h}{C}, \quad \bar{p} = \frac{pC^2}{\mu \omega R^2}, \\ l_m = \frac{C}{\Lambda}, \quad \bar{\alpha} = \frac{\alpha}{C}, \quad \bar{\sigma} = \frac{\sigma}{C}, \quad \bar{\xi} = \frac{\xi}{C^3} \quad (7)$$

$$\frac{\partial}{\partial \theta} \left[ \bar{F}(N, \bar{l}_m, \bar{h}, \bar{\alpha}, \bar{\sigma}, \bar{\xi}) \frac{\partial \bar{p}}{\partial \theta} \right] + \frac{1}{(L/D)^2} \frac{\partial}{\partial \bar{z}} \left[ \bar{F}(N, \bar{l}_m, \bar{h}, \bar{\alpha}, \bar{\sigma}, \bar{\xi}) \frac{\partial \bar{p}}{\partial \bar{z}} \right] = \frac{\partial \bar{h}}{\partial \theta} \quad (8)$$

Where,

$$\bar{F}(N, \bar{l}_m, \bar{h}, \bar{\alpha}, \bar{\sigma}, \bar{\xi}) = \frac{1}{C^3} F(\Lambda, N, H) \\ = \bar{h}^3 + \bar{\alpha}^3 + \bar{\xi} + 3\bar{h}^2\bar{\alpha} + 3\bar{h}\bar{\alpha}^2 + 3\bar{h}\bar{\sigma}^2 + 3\bar{\alpha}\bar{\sigma}^2$$

$$+ \frac{12(\bar{h} + \bar{\alpha})}{\bar{l}_m^2} - \frac{6N}{\bar{l}_m} (\bar{\sigma}^2 + \bar{h}^2 + \bar{\alpha}^2 + 2\bar{h}\bar{\alpha})$$

$$\coth \frac{N \bar{l}_m (\bar{h} + \bar{\alpha})}{2} \quad (9)$$

Eq. (8) represents the modified Reynolds equation of rough hydrodynamic journal bearing under micropolar lubrication its non-dimensional form.

As per the configuration of a journal bearing (Fig.1), as the expression of non-dimensional thickness of fluid film  $\bar{h}$  is a function of  $\varepsilon_0$ ,  $\bar{F}$  will also be a function of  $\varepsilon_0$ . Hence eq. (8) can be expressed as:

EFFECT OF SURFACE ROUGHNESS ON THE PRESSURE GENERATION

$$\bar{F} \frac{\partial^2 \bar{p}}{\partial \theta^2} + \frac{\partial \bar{F}}{\partial \theta} \frac{\partial \bar{p}}{\partial \theta} + \frac{1}{(L/D)^2} \left[ \bar{F} \frac{\partial^2 \bar{p}}{\partial \bar{z}^2} \right] = 6 \frac{\partial \bar{h}}{\partial \theta} \quad (10)$$

**Boundary condition:**

1. The pressure distribution bears a reflection symmetry along the journal axis over the mid-plane of the bearing

$$\frac{\partial \bar{p}(\theta, 0)}{\partial \bar{z}} = 0$$

2. The pressures at the ends of the bearing are zero *i.e.*

$$\{\bar{p}(\theta, \bar{z})\}_{\bar{z}=+1} = \{\bar{p}(\theta, \bar{z})\}_{\bar{z}=-1} = 0$$

3. Cavitations boundary condition as stated by Floberg [15]:

$$\left( \frac{\partial \bar{p}}{\partial \theta} \right)_{\text{at } \theta_2, \bar{z}} = 0 \quad \text{And} \quad \bar{p}(\theta, \bar{z}) = 0 \quad \text{for} \quad \theta_2 \leq \theta \leq \theta_1$$

Where,  $\theta_1$  and  $\theta_2$  represents the angular positions where the film starts and cavitates.

**Numerical Solution:**

The finite difference method is applied for the solution considering rectangular meshes of size

$(\Delta\theta \times \Delta\bar{z})$  each in which the first and second order derivatives of non-dimensional pressure  $\bar{p}$  and the micropolar function  $\bar{F}$  are represented by central difference method as follows:

$$\left. \begin{aligned} \frac{\partial \bar{p}}{\partial \theta} &= \frac{(\bar{p})_{i+1,j} - (\bar{p})_{i-1,j}}{2(\Delta\theta)} & \frac{\partial \bar{p}}{\partial \bar{z}} &= \frac{(\bar{p})_{i,j+1} - (\bar{p})_{i,j-1}}{2(\Delta\bar{z})} \\ \frac{\partial \bar{F}}{\partial \theta} &= \frac{(\bar{F})_{i+1,j} - (\bar{F})_{i-1,j}}{2(\Delta\theta)} & \frac{\partial \bar{F}}{\partial \bar{z}} &= \frac{(\bar{F})_{i,j+1} - (\bar{F})_{i,j-1}}{2(\Delta\bar{z})} \\ \frac{\partial^2 \bar{p}}{\partial \theta^2} &= \frac{(\bar{p})_{i+1,j} - 2(\bar{p})_{i,j} + (\bar{p})_{i-1,j}}{(\Delta\theta)^2} & \frac{\partial^2 \bar{p}}{\partial \bar{z}^2} &= \frac{(\bar{p})_{i,j+1} - 2(\bar{p})_{i,j} + (\bar{p})_{i,j-1}}{(\Delta\bar{z})^2} \end{aligned} \right\} \quad (12)$$

With the above finite difference scheme the non-dimension pressure at every grid point is obtained by expanding eq. (10) as follows:

$$(\bar{p})_{i,j} = C_1 (\bar{p})_{i+1,j} + C_2 (\bar{p})_{i-1,j} + C_3 (\bar{p})_{i,j+1} + C_4 (\bar{p})_{i,j-1} + C_5 \quad (13)$$

$$\text{Where, } C_0 = 2 \left[ 1 + \frac{1}{(L/D)^2} \left( \frac{\Delta\theta}{\Delta\bar{z}} \right)^2 \right]$$

$$C_1 = \frac{1}{C_0} \left( 1 + \frac{CF_1}{4} \right)$$

$$\text{and } C_2 = \frac{1}{C_0} \left( 1 - \frac{CF_1}{4} \right)$$

$$C_3 = \frac{1}{C_0(L/D)^2} \left( \frac{\Delta\theta}{\Delta\bar{z}} \right)^2$$

$$\text{and } C_4 = \frac{1}{C_0(L/D)^2} \left( \frac{\Delta\theta}{\Delta\bar{z}} \right)^2$$

$$C_5 = \frac{6 \varepsilon_0 (\Delta\theta)^2}{C_0 (\bar{F})_{i,j}} \sin \theta_i$$

$$\text{In which, } CF_1 = \frac{(\bar{F})_{i+1,j} - (\bar{F})_{i-1,j}}{(\bar{F})_{i,j}}$$

(14)

**Table 1. Comparison of the result obtained in the ongoing study with those obtained by S. Das[6]**

	Newtonian	$N^2 = 0.1,$ $l_m = 10.0$	$N^2 = 0.5,$ $l_m = 10.0$	$N^2 = 0.9,$ $l_m = 10.0$	$N^2 = 0.3,$ $l_m = 1.0$	$N^2 = 0.3,$ $l_m = 10.0$	$N^2 = 0.3,$ $l_m = 30.0$
$\bar{p}_{\max}$ obtained in ongoing study	1.93268 at 142.5°	2.12732 at 142.5°	3.03422 at 142.5°	4.50274 at 150.0°	2.75726 at 142.5°	2.54267 at 142.5°	2.21738 at 142.5°
$\bar{p}_{\max}$ obtained by Das, S. [6]	1.93027 at 142.5°	2.12469 at 142.5°	3.0305 at 142.5°	4.49757 at 150.0°	2.75382 at 142.5°	2.54131 at 142.5°	2.21464 at 142.5°

All  $\bar{p}_{\max}$  have occurred at the midplane of the journal.

Eq. (13) is then solved with successive over relaxation scheme as discussed by Castelli *et al.* [16] with the help of the boundary condition as stated in eq.(11) and the convergence criteria  $\left| \frac{\sum p^{n+1} - \sum p^n}{\sum p^{n+1}} \right| \leq 0.001$ , and taking over-relaxation factor as 1.03.

### 3. RESULTS AND DISCUSSION

The results obtained in this study for a smooth journal-bearing system is compared with the results obtained by S. Das[6] and is presented in Table 1, that validates the theory and computer code developed In this analysis, the film pressure  $\bar{p}$  under steady state condition is found to depend on the characteristics of lubricating fluid, *i.e.* the micropolar parameters— Coupling number ( $N$ ) and non dimensional characteristic length ( $l_m$ ), the geometric parameters— eccentricity ratio ( $\varepsilon_\rho$ ), slenderness ratio ( $L/D$ ) and the Stochastic roughness part of the fluid film *i.e.*  $h_s$  which as per roughness model considered can be expressed through three statistical parameters *viz.* the mean ( $\bar{\alpha}$ ), standard deviation ( $\bar{\sigma}$ ) and skewness ( $\bar{\xi}$ ). The detailed study on pressure profile is therefore done and presented for those parameters. Respective film pressure generations in Newtonian lubrication are also studied for the comparison with the results of the micropolar fluid.

#### 3.1. Effect of Coupling Number ( $N$ )

Effect of coupling number ( $N$ ) on non-dimensional pressure profile is shown through Figs. 2 to 5 for increasing values of  $N$ , keeping other values fixed at  $l_m = 10.0$ ,  $L/D = 1.0$ ,  $\varepsilon_\rho = 0.5$  and non-dimensional values of roughness parameters *viz* mean, standard deviation and skewness as  $\bar{\alpha} = 0.1$ ,  $\bar{\sigma} = 0.1$  and  $\bar{\xi} = 0.01$ . Fig.6 shows the pressure profile at the mid-plane of the bearing, which also is the position of the peak pressure due to the reflection symmetry of the system over the mid-plane of the bearing for parametric variation of  $N$  keeping other parameters same as before. The figures show that the three-dimensional structure of the pressure profiles though are similar, the pressure generated at every grid point increases as the coupling number is increased. Coupling number ( $N$ ) couples the translation and rotational momentum arising as the result of the microspin effect of the micropolar particles in the fluid; thus results the generation of an extra viscosity  $\chi$  which is called the spin viscosity of the micropolar fluid. As  $\chi$  increases with increase in  $N$ , the effective viscosity gradually increases from the Newtonian value as  $N$  increases. This enables the fluid to generate higher pressure as the coupling number enhances. On the other hand as  $N = 0$ ,  $\chi = 0$ , the equations representing linear and angular momentums become uncoupled resulting eq. (7) to reduce to that of classical steady state Reynolds equation.

EFFECT OF SURFACE ROUGHNESS ON THE PRESSURE GENERATION

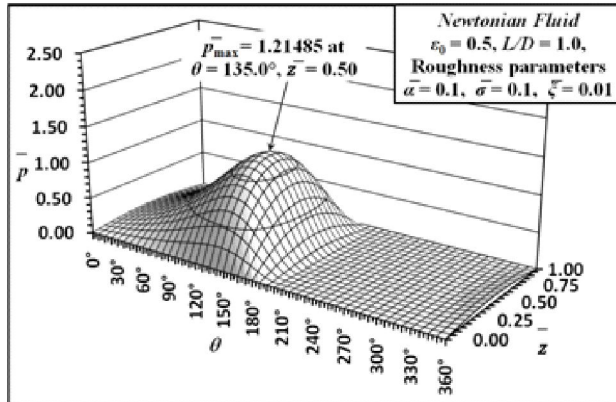


Fig.2. Pressure profile for the Newtonian fluid.

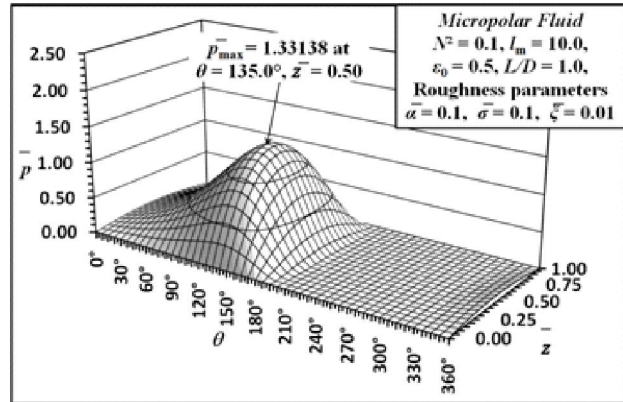


Fig.3. Pressure profile for  $N^2 = 0.1$ .

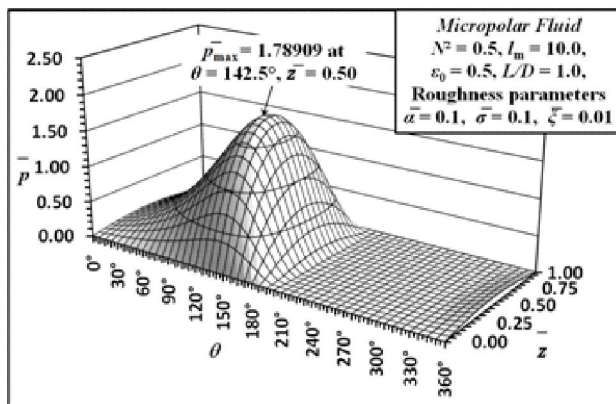


Fig.4. Pressure profile for  $N^2 = 0.5$ .

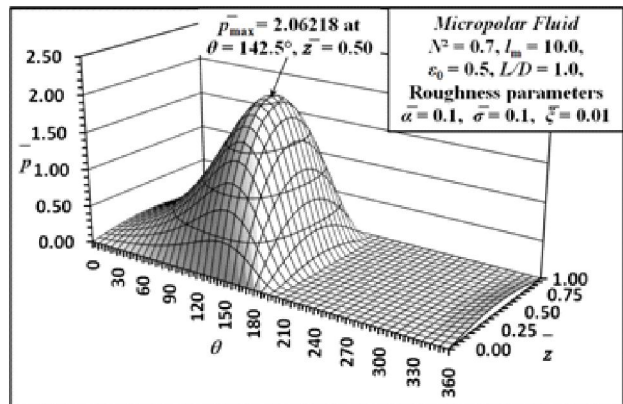


Fig.5. Pressure profile for  $N^2 = 0.7$ .

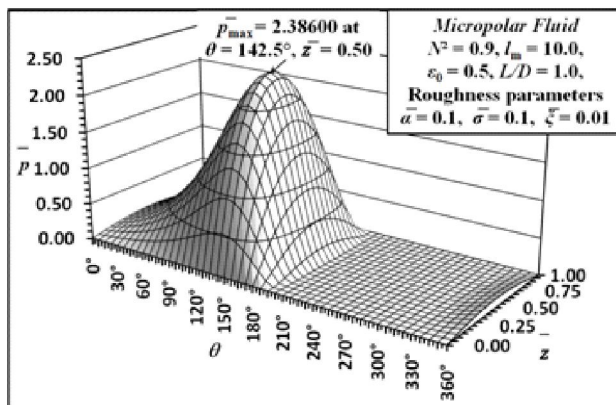


Fig.6. Pressure profile for  $N^2 = 0.9$ .

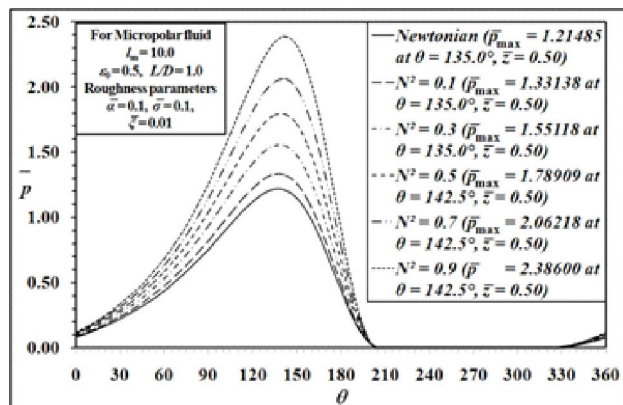


Fig.7. Pressure profile at the mid-plane for varying  $N$ .

**3.2. Effect of Non-dimensional Characteristic Length ( $l_m$ )**

The effect of  $l_m$  is observed in the series of figure Figs. 8 to 13 along with Fig. 2 for  $N^2 = 0.3$ ,  $\epsilon_0 = 0.5$ ,  $L/D = 1.0$  and  $\bar{\alpha} = 0.1$ ,  $\bar{\sigma} = 0.1$  and  $\bar{\zeta} = 0.01$ .

Fig. 8 to Fig. 12 and Fig. 2 show that the pressure generation is gradually drooping down to the Newtonian value as  $l_m$  is increased. The strong micropolar effect is evitable with the enhancement in the value of characteristic length ( $l_m$ ) or

decrease in clearance in between the journal and bearing (C) i.e. with the fall in the value of non-dimensional characteristic length  $l_m$ . So the effect of  $l_m$  is very important in lubrication theory as C is usually very small here. In the limiting situation

when  $l_m \rightarrow \infty$ ,  $\lambda \rightarrow 0$  the micropolar effect is diminished and the lubrication problem diminishes to a Newtonian lubrication. Hence the pressure generation gradually reduces to the Newtonian value as  $l_m$  increases.

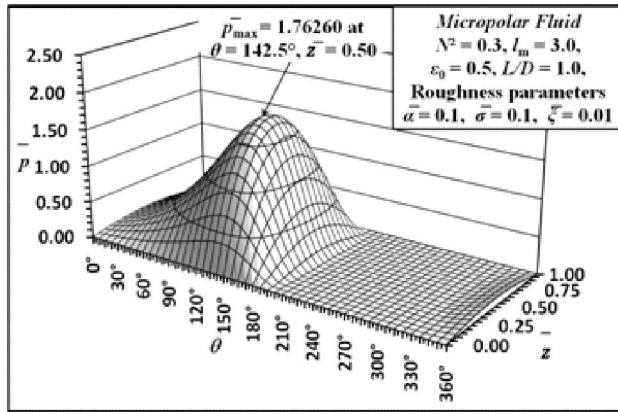


Fig.8. Pressure profile for  $l_m = 3.0$ .

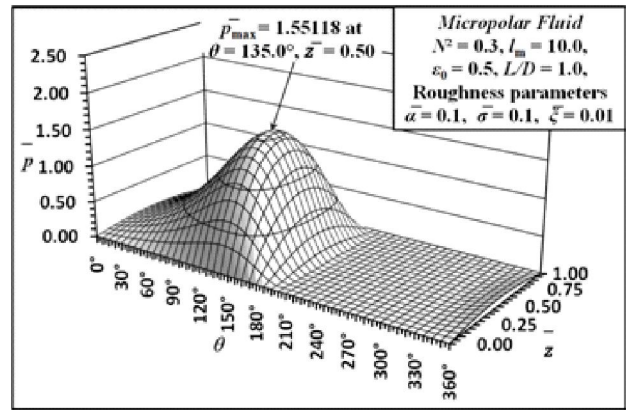


Fig.9. Pressure profile for  $l_m = 10.0$ .

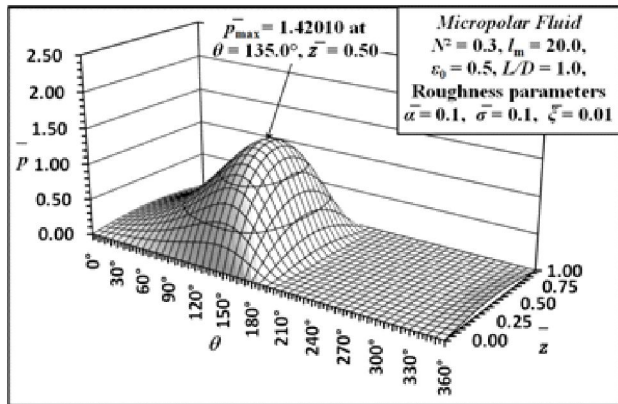


Fig.10. Pressure profile for  $l_m = 20.0$ .

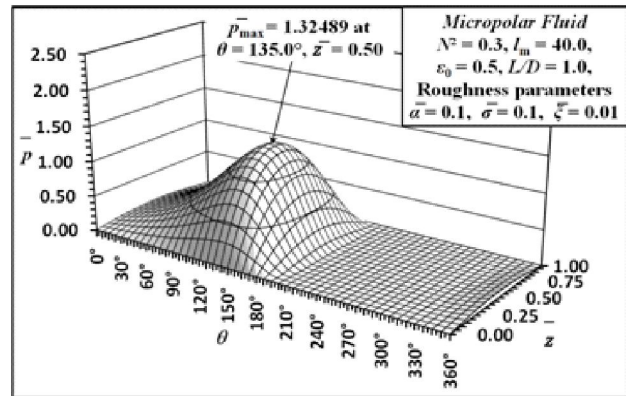


Fig.11. Pressure profile for  $l_m = 40.0$ .

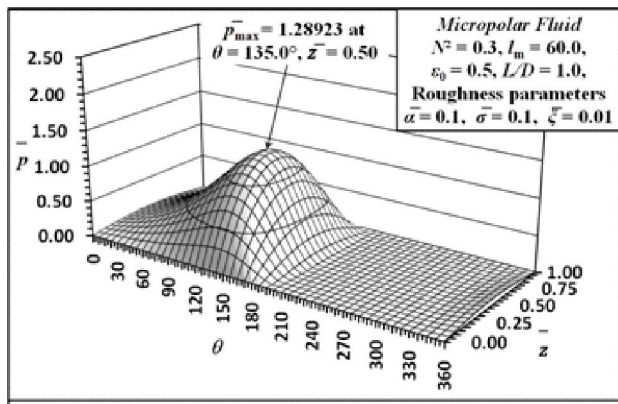


Fig.12. Pressure profile for  $l_m = 60.0$ .

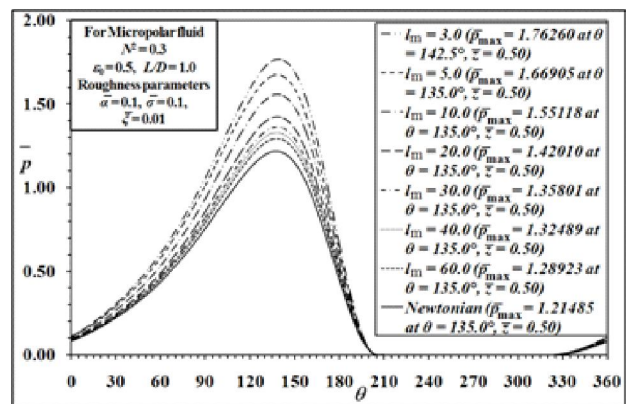


Fig.13. Pressure profile at the mid-plane for varying  $l_m$ .

**3.3. Effect of Non-dimensional Mean ( $\bar{\alpha}$ ) of the roughness**

Variation of pressure profile at the bearing's mid-plane for the parametric variation of non-dimensional mean ( $\bar{\alpha}$ ) of roughness model is presented in Fig. 14 for in the range  $[-0.10, 0.10]$  keeping  $\varepsilon_0 = 0.5$ ,  $L/D = 1.0$ ,  $\bar{\sigma} = 0.1$ , and  $\bar{\xi} = 0.01$  for both Newtonian and micropolar lubricants. For micropolar fluid  $l_m$  and  $N^2$  are taken as 10.0 and 0.5 respectively. The peak pressures and its points of occurrence are summarized in the figure, which establishes that pressure generation in micropolar lubricant always exceeds the pressure in the Newtonian fluid. The peak pressure always generates at the mid-plane as expected, though it occurs a little away in the angular position in micropolar fluid than that in the

Newtonian fluid. As the  $\bar{\alpha}$  shifts from the negative maximum to the positive maximum in the range the pressure generation gradually is decreased. This is because the average film thickness gradually decreases as  $\bar{\alpha}$  increases in its range. With same value of  $\bar{\alpha}$ , pressure generation in micropolar fluid also is higher in comparison to the Newtonian fluid. Change of  $\bar{\alpha}$  has no effect on the position of  $\bar{p}_{max}$ . The combined effect of micropolar parameters  $N$  and  $l_m$  along with  $\bar{\alpha}$  are shown in Figs. 15 and 16 respectively. In both cases pressure generation decrease as  $\bar{\alpha}$  increases as the local film thickness decrease. Again  $\bar{p}$  approaches gradually to its Newtonian value as the micropolar effect gradually diminishes *i.e.* as  $N$  decreases or  $l_m$  increases.

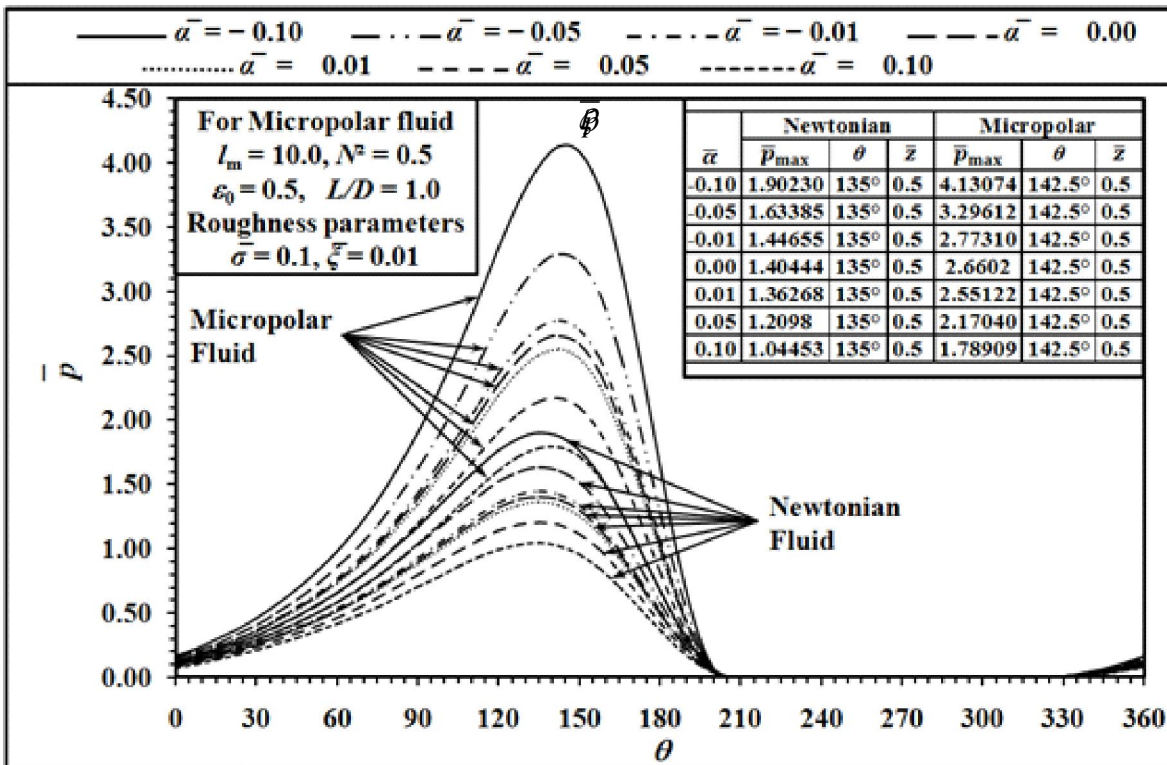


Fig.14. Pressure profile at the mid-plane for varying Non-dimensional Mean  $\bar{\alpha}$  of the roughness model.

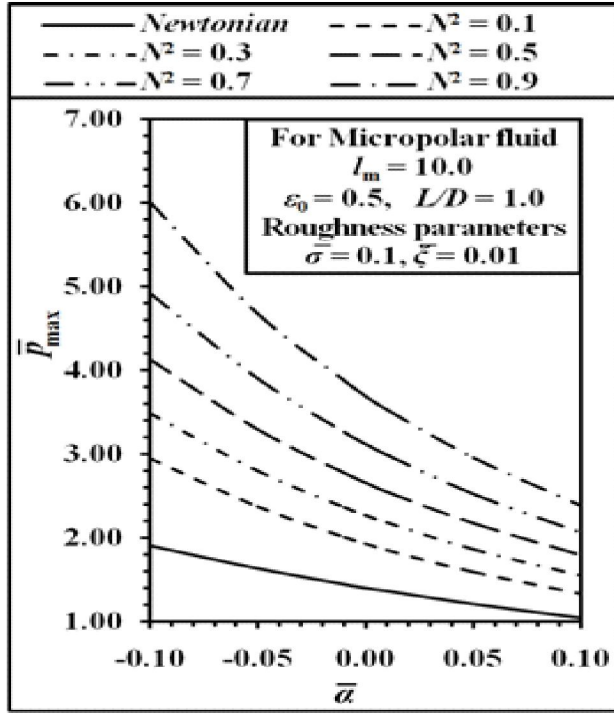


Fig.15. Variation of peak pressure with  $\bar{\alpha}$  for varying  $N$ .

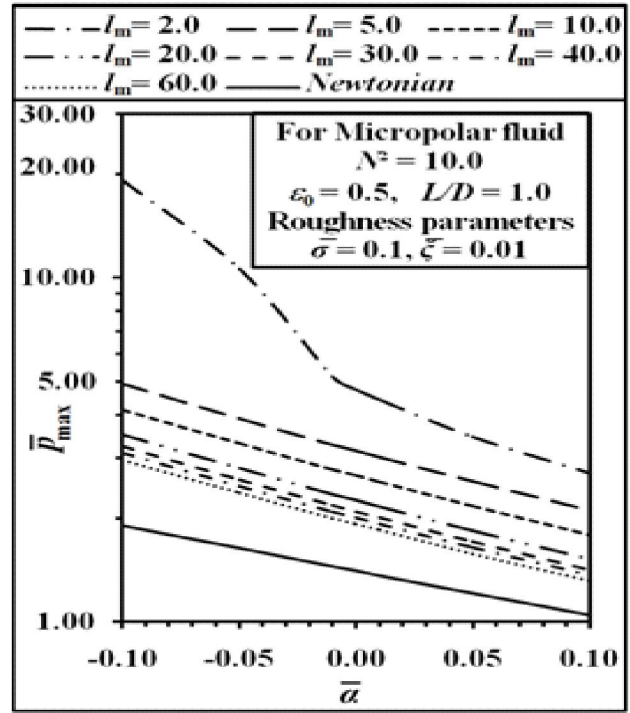


Fig.16. Variation of peak pressure with  $\bar{\alpha}$  for varying  $l_m$ .

### 3.4. Effect of Non-dimensional Standard Deviation ( $\bar{\sigma}$ ) of the roughness

Fig. 17 exhibits the effect of non-dimensional standard deviation ( $\bar{\sigma}$ ) of roughness model on pressure generation for  $\epsilon_0 = 0.5$ ,  $L/D = 1.0$ ,  $\bar{\alpha} = 0.1$  and  $\bar{\zeta} = 0.01$  for both Newtonian and micropolar lubricant. For micropolar fluid  $l_m$  and  $N^2$  are chosen as 5.0 and 0.5 respectively. The values of  $\bar{p}_{max}$  are mentioned in the figure with their points of occurrence. It is observed that  $\bar{p}$  is always high in the micropolar fluid in comparison to the Newtonian fluid in the same operating condition. The peak pressure again generates at the midplane and a little further angular position in micropolar fluid than that in the Newtonian fluid.  $\bar{p}$  drops in both lubricants with the increase in  $\bar{\sigma}$ . This is because the increase of  $\bar{\sigma}$  for a

particular  $\bar{\alpha}$  indicates acceptance of wider range of roughness over the specified mean  $\bar{\alpha}$  resulting the increase in average fluid film thickness. In Fig. 18 and Fig. 19 the combined effect of  $N$ ,  $\bar{\sigma}$  and  $l_m$ ,  $\bar{\sigma}$  are presented, which show that the pressure generation gradually falls to its Newtonian values as the effect of micropolarity diminishes. Both curves show increase in pressure with a decreasing rate as  $\bar{\sigma}$  decreases. This also can be explained by the fact that as  $\bar{\sigma}$  decreases the roughness approaches slowly to its mean value, resulting the film to converge to its minimum value slowly for that  $\bar{\alpha}$ . This is because as variance decreases the local film thicknesses not only increases but also gradually stabilizing to a value corresponding to the mean value of the roughness considered.

EFFECT OF SURFACE ROUGHNESS ON THE PRESSURE GENERATION

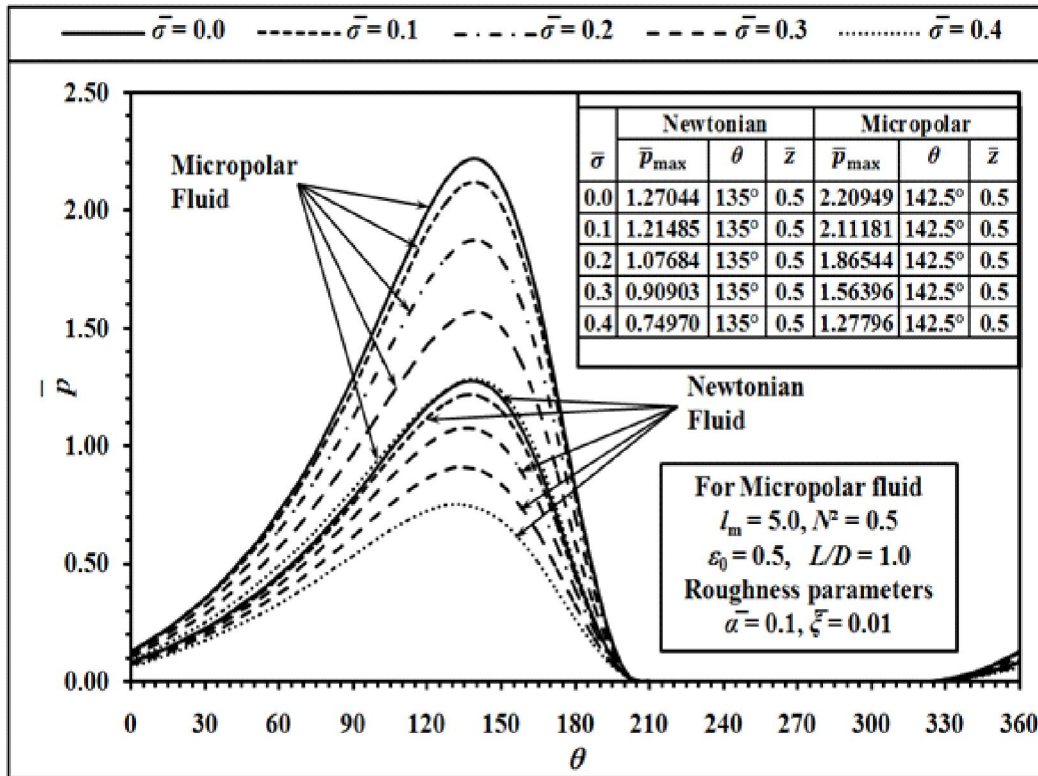


Fig.17. Pressure profile at the mid-plane for varying Non-dimensional Standard Deviation  $\bar{\sigma}$  of the roughness model.

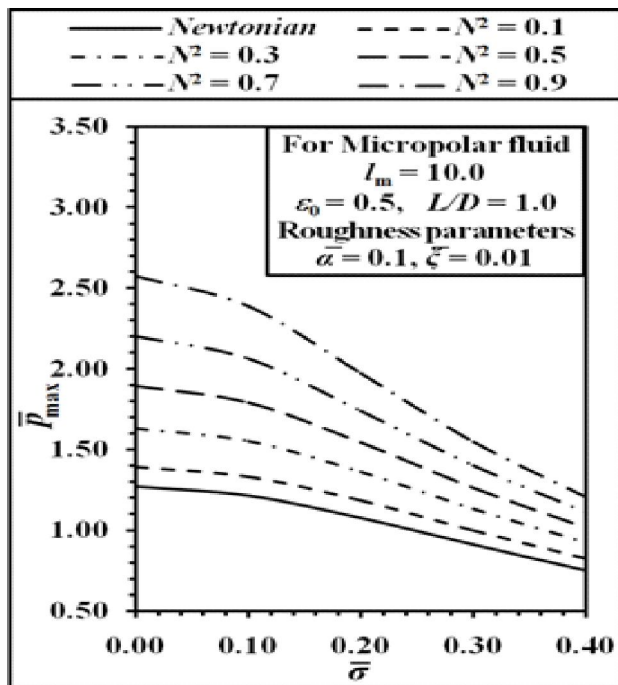


Fig.18. Variation of peak pressure with  $\bar{\sigma}$  for varying  $N$ .

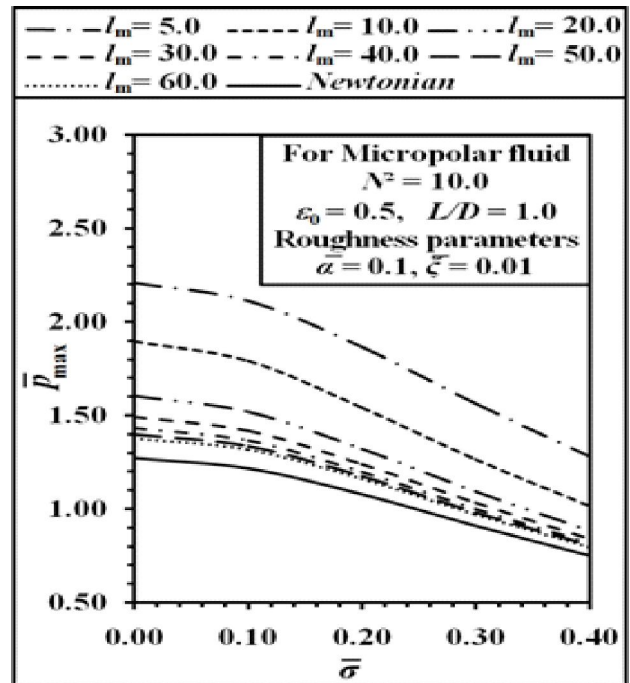


Fig.19. Variation of peak pressure with  $\bar{\sigma}$  for varying  $l_m$ .

### 3.5. Effect of Non-dimensional Skewness ( $\bar{\xi}$ ) of the roughness

Effect of skewness of the roughness model on the film pressure under both lubrications are shown in Fig. 20 for the range  $-0.01 \leq \bar{\xi} \leq 0.10$  and the combined effects of  $N$  and

$l_m$  along with  $\bar{\xi}$  are presented in respective Figs. 21 and 22. Fig. 20 exhibits similarity with Fig. 17 and Figs. 21, 22 shows the similar trend as exhibited in Figs. 15, 16. This is because as the skewness increases the average film thickness decreases resulting lower pressure generation.

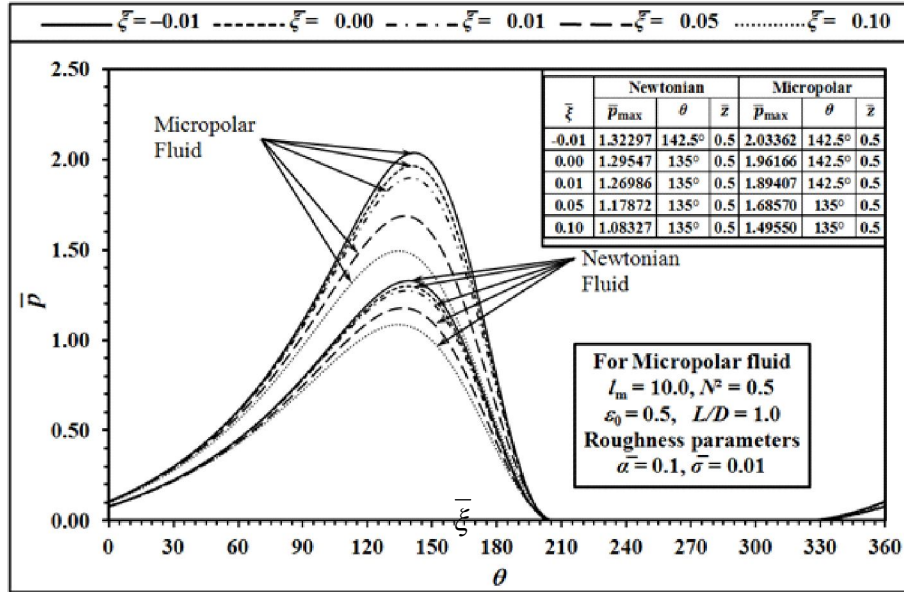


Fig.20. Pressure profile at the mid-plane for varying Non-dimensional Standard Deviation  $\bar{\sigma}$  of the roughness model.

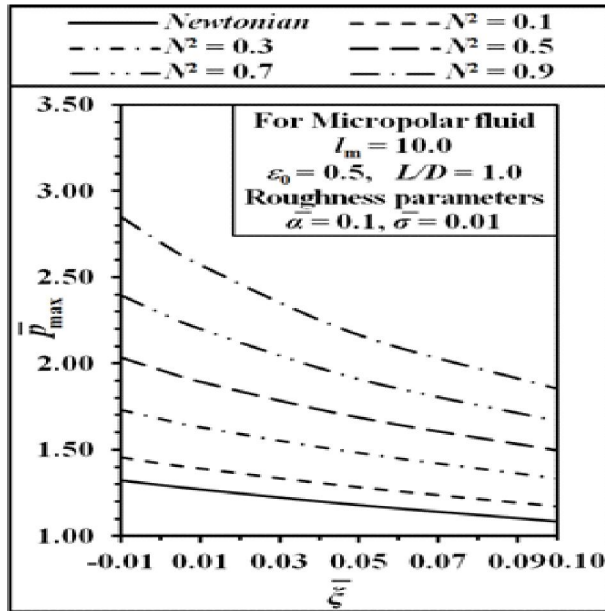


Fig.21. Variation of peak pressure with  $\bar{\xi}$  for varying  $N$ .

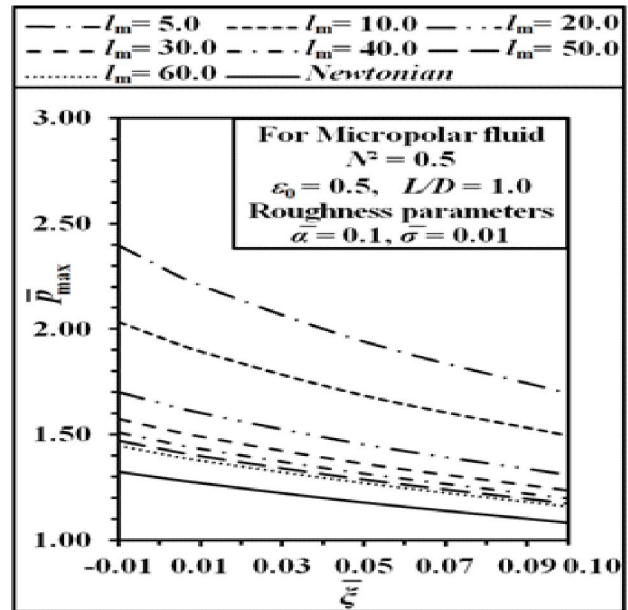


Fig.22. Variation of peak pressure with  $\bar{\xi}$  for varying  $l_m$ .

#### 4. Conclusion

- The steady state pressure is always higher in micropolar fluid than that in Newtonian fluid and it increases with the increase in the degree of micropolarity *i.e.* with increase in  $N$  and decrease in  $l_m$ , because in such cases the degree of micropolarity enhances resulting generation of higher effective viscosity.
- The steady state pressure decreases with the increase in the mean of surface roughness ( $\bar{\alpha}$ ), standard deviation ( $\bar{\sigma}$ ) and skewness of roughness model ( $\bar{\xi}$ ), as increase in the values of each of these parameters result the decrease in the steady state film thickness.

#### Reference

- [1] Eringen, A.C., Theory of Micropolar Fluids, J. Math. Mech., Vol.16, No.1, pp.1-18, 1966.
- [2] Prakash, J. and Sinha, P., Lubrication Theory for Micropolar Fluids and Its Application to a Journal Bearing, Int. J. Engng. Sci., Vol.13, pp.217-232, 1975.
- [3] Tipei, N., Lubrication with Micropolar Liquids and Its Application to Short Bearings, J. Lub. Technol., Trans. ASME, Vol.101, Jul., pp.356-363, 1979.
- [4] Singh, C. and Sinha, P., The Three-Dimensional Reynolds Equation for Micropolar Fluid Lubricated Bearings, Wear, Vol.76, No.2, pp.199-209, 1982.
- [5] Khonsari, M.M. and Brewster, D.E., On the Performance of Finite Journal Bearings Lubricated with Micropolar Fluids, STLE Tribology Transactions, Vol.32, No.2, pp.155-60, 1989.
- [6] Das, S., Steady State and Dynamic Analysis including Stability of Hydrodynamic Journal Bearings with Micropolar Lubrication, Doctoral Thesis, Bengal Engineering and Science University, Shibpur, 2004.
- [7] Hamilton, D.B., Walowit, J.A. and Allen, C.M., A Theory of Lubrication by Microirregularities, J. Basic Engng., Trans ASME, Ser. D., Vol.88, No.1, pp.177-185, 1966.
- [8] Christensen, H., Stochastic Models for Hydrodynamic Lubrication of Rough Surfaces, Proc. Instn. Mech. Engrs., Vol.184, pp.1013-1025, 1969.
- [9] Christensen, H. and Tonder, K., The Hydrodynamic Lubrication of Rough Journal Bearings, Trans. ASME, J. of Lubr. Tech., Series F, April, pp.166-170, 1973.
- [10] Guha, S.K., Analysis of Steady-State Characteristic of Misaligned Hydrodynamic Journal Bearings with Isotropic Roughness Effect, Trib. Int., Vol.33, No.1, pp.1-12, 2000.
- [11] Cheng-I, Weng and Chien-Ru C., Linear Stability of Short Journal Bearings with Consideration of Flow Rheology and Surface Roughness, Trib. Int., Vol.34, No.1, pp.507-516, 2001.
- [12] Rao, P.S. and Agarwal, S., Effect of Surface Roughness on the Hydrodynamic Lubrication of Porous Inclined Slider Bearing Considering Slip Velocity and Squeeze Velocity with Couple Stress Fluids, Int. J. Engng. Sc. and Tech., Vol.6, No.2, pp. 45-64, 2014.
- [13] Mishra, P.C., Analysis of a Rough Elliptic Bore Journal Bearing using Expectancy Model of Roughness Characterization, Trib. in Industry, Vol. 36, No. 2, pp.211-219, 2014.
- [14] Yan, X-L., Wang, X-L and Zhang, Y-Y., Influence of Roughness Parameters Skewness and Kurtosis on Fatigue Life Under Mixed Elastohydrodynamic

- Lubrication Point Contacts, *J. Tribol.*, ASME, Vol. 136, No. 3, 2014.
- [15] Floberg, L., Boundary Condition of Cavitation Regions in Journal Bearings, *ASLE Trans.*, Vol.4, pp.282–286, 1961.
- [16] Castelli, V., Stevenson, C.H. and Gunter, E.J., Steady-state Characteristic of Gas lubricated Self-acting Partial-arc Journal Bearings of Finite Width, *Trans., ASLE.*, Vol.7, pp.153–167, 1964.
- [17] Dowson D., Developments in Lubrication – the Thinning Film, *J. Phys. D, Appl Phys*, Vol.25, Ser.A, pp.334–339, 1992.